Talanta 129 (2014) 86–92

Contents lists available at ScienceDirect

Talanta

journal homepage: www.elsevier.com/locate/talanta

Non-covalent conjugation of CdTe QDs with lysozyme binding DNA for fluorescent sensing of lysozyme in complex biological sample

Shujia Li, Zhidan Gao, Na Shao*

College of Chemistry, Beijing Normal University, Beijing 100875, PR China

ARTICLE INFO

Article history:
Received 16 February 2014
Received in revised form
15 April 2014
Accepted 21 April 2014
Available online 2 May 2014

Keywords:
Lysozyme
CdTe quantum dots
Label-free
Lysozyme binding DNA
Fluorescence enhancement

ABSTRACT

Water-soluble cysteamine (CA) capped CdTe quantum dots (QDs) conjugated with lysozyme binding DNA (LBD) was constructed for luminescent sensing of lysozyme by forming a ternary self-assembly complex. Addition of negatively charged lysozyme binding DNA to the positively charged CA capped CdTe QDs buffer solution (Tris–HCl pH 7.4) could lead to the formation of QDs–LBD complex through electrostatic interactions. Once lysozyme was introduced into the CdTe QDs–LBD system, it could bind specifically with the QDs–LBD complex, resulting in fluorescence emission enhancement of the QDs due to the surface inert of QDs. At a given amount of LBD and CdTe QDs (LBD: QDs=2: 1), the fluorescence intensity enhancement of QDs was linear with lysozyme concentration over the range of 8.9–71.2 nM, with a detection limit of 4.3 nM. Due to the specific binding of LBD with lysozyme, this approach displayed high selectivity for lysozyme recognition. The sensing mechanism was confirmed by DLS and zeta potential measurement, and agarose gel electrophoresis experiment. Furthermore, the proposed CA–capped CdTe QDs–LBD sensor was applied to lysozyme detection in mouse serum and human morning urine samples, which showed high sensitivity and selectivity in the complex biological sample.

1. Introduction

Lysozyme is a ubiquitous protein in mammals and is often termed “body's own antibiotic”. in vivo, lysozyme is an important defense molecule of the innate immune system and the lysozyme level in serum and urine could be used as clinical index for many diseases, such as leukemia and renal diseases [1,2]. It has been discovered recently that antibodies against citrullinated variants of lysozyme are present in patients with rheumatoid arthritis [3] which highlights the qualitative and quantitative determination of lysozyme are useful in the diagnosis, treatment and monitoring the progression of some diseases. Due to its biological significances, extensive efforts have been devoted to develop simple and sensitive approach for the detection of the protein.

Oligonucleotide which are specific to amino acids, drugs, proteins and other molecules, was named as aptamer [4,5] or binding DNA [6,7]. This type of oligonucleotide offers several advantages over traditional antibodies, owing to their relative ease of isolation and modification, tailored binding affinity, and resistance against denaturizing. Many oligonucleotide aptamers have been broadly used in the detection of drugs and a variety of proteins [8–11]. In 2001, Ellington et al. developed an anti-lysozyme RNA aptamer from a DNA template using automated nucleic acid selection methods [12]. Later on, the DNA template of the lysozyme RNA aptamer was widely used by many researchers to construct aptamer-based biosensors for lysozyme. Wang's group used this derived DNA aptamer to construct electrochemical biosensor for lysozyme [13,14]. This derived DNA aptamer was also successfully used by Yu et al. for voltammetric detection of lysozyme [15]. In recent years, many reported methods, such as fluorescence spectroscopy [16–20], electrochemistry [21–25], electrochemiluminescence (ECL) [26,27], and so on [28–35], indicated that this derived DNA aptamer could be used for specific recognition of lysozyme. Willson [36] and Sim [37] also proved that this derived DNA aptamer used in the above mentioned studies has high and specific binding ability for lysozyme.

However, in most of the reported aptamer-based lysozyme assays, the derived DNA aptamer were either covalently conjugated to fluorophores [16–20] or fixed onto a certain surface like electrodes [21–23,25,27]. Such covalent modifications are usually time-consuming and labor-intensive, and more important, would decrease the binding abilities of the drived DNA aptamer toward their targets [38–40].

In this paper, we proposed herein an alternative approach for fluorescent sensing of lysozyme using a complex fluorescent probe formed by CdTe QDs and the derived DNA aptamer (here we called it lysozyme binding DNA, LBD) used by Wang et al. [13].

* Corresponding author. Fax: +86 10 58802146.
E-mail address: shaona@bnu.edu.cn (N. Shao).

http://dx.doi.org/10.1016/j.talanta.2014.04.062
0039-9140/

This method worked on fluorescence "turn-on" mode by forming a self-assembly ternary complex between QDs–LBD and lysozyme. The QDs–LBD complex was formed based on electrostatic interactions between positively charged CA–QDs and negatively charged LBD, and the covalent immobilization of LBD molecule onto the surface of QDs is not required. The electrostatic coupling made the QDs–LBD complex more stable and present a red-shift of the maximum emission wavelength compared with native CdTe QDs. When lysozyme was introduced into the QDs–LBD system, the fluorescence of CdTe QDs enhanced significantly due to the binding of lysozyme with QDs–LBD forming a ternary complex. Thus, the specific recognition of lysozyme can be achieved via monitoring the fluorescence signal enhancement of QDs. The detection of lysozyme in mouse serum and human urine sample by this sensing platform was also demonstrated, which showed highly sensitive and selective response to lysozyme even in complex biological matrix.

2. Experimental

2.1. Chemicals and apparatus

All reagents are of analytical grade and used without further purification. $CdCl_2 \cdot 2.5H_2O$ (Alfa-Aesar), Tellurium powder (Alfa-Aesar) and $NaBH_4$ (sinopharm chemical reagent company) were used to prepare CdTe QDs. Cysteamine hydrochloride (CA) (J&K Chemical) was used as the capping agent. Lysozyme, bovine serum albumin (BSA), immunoglobin G (IgG), thrombin, trypsin, histidine, arginine, serine, proline, glycine and L-lysine were purchased from Beijing Dingguo Biotechnology Company. The 42-mer lysozyme binding DNA (LBD) with the sequence of 5′-ATC TAC GAA TTC ATC AGG GCT AAA GAG TGC AGA GTT ACT TAG-3′ was synthesized by Beijing Dingguo Biotechnology Company and dissolved in 20 mM Tris–HCl buffer (pH 7.4) containing 0.1 M NaCl and 5 mM $MgCl_2$ for annealing [14]. Fresh mouse serum was also purchased from Beijing Dingguo Biotechnology Company. The original serum was centrifuged three times (5000 rpm, 10 min each time) and then the supernatant was extracted. The serum samples were diluted 30 times prior to detection. The urine sample was freshly taken from human. Aqueous solutions of Na^+, K^+, Ca^{2+} and Fe^{3+} were prepared from NaCl, KCl, $CaCl_2$ and $Fe(NO_3)_3 \cdot 9H_2O$, respectively. Ultrapure water (over 18 MΩ cm) from a Milli-Q Reference system (Millipore) was used throughout. Absorbance measurements were performed using a TU-1901 diode-array spectrophotometer. Fluorescence spectra and fluorescence anisotropy were recorded using Hitachi F-4600. Transmission electron microscopy (TEM) graphs were obtained using a TF20 (FEI). Dynamic light scattering (DLS) and Zeta potential measurements were performed with the Brookhaven Zeta Potential Analyzer. Gel electrophoresis was performed on a DYY-6C electrophoresis apparatus. The pH of buffer solution was determined by a REX PHS-3C pH meter. A stirrer with temperature sensor and a thermometer was used to control the temperature precisely.

2.2. Synthesis of CA–CdTe QDs

The CA–CdTe QDs were synthesized according to the previously reported literature with minor modification [41]. Briefly, under a N_2 atmosphere, absolute ethanol (3 mL) was added to the prepared tellurium (6.8 mg) and excess sodium borohydride (20 mg) mixture under magnetic stirring, which was then kept at 70 °C for 1.0 h. The resulting produced colorless ethanol solution of NaHTe was reacted with H_2SO_4 (50 mM, 5 mL) to generate H_2Te gas. Under stirring, H_2Te gas was introduced into the oxygen-free $CdCl_2$ (3.0 mM, 50 mL) aqueous solution containing cysteamine hydrochloride (15 mM, 30 mg) stabilizer at pH 5.7 with a slow N_2 flow for 15 min. CdTe precursors are formed at this stage accompanied by a color change of the solution from colorless to dark-red. The precursors were converted to CdTe nanocrystals by refluxing the reaction mixture at 100 °C for 3 h under open-air conditions with condenser attached. The molar ratio of Cd^{2+}/Te^{2-}/CA was fixed at 3: 1: 5 in the whole reaction.

2.3. Preparation of the QDs–LBD complex

The LBD (100 μM) was first heated at 70 °C in incubation buffer (20 mM Tris, 0.1 M NaCl, 5 mM $MgCl_2$, pH 7.4) for 4 min, and then left to slowly cool down to room temperature. The QDs–LBD complex was prepared by mixing CA–QDs (with final concentration of 200 nM) with LBD (with final concentration of 400 nM) in Tris–HCl buffer. The 1: 2 ratios of QDs to LBD ensured stable structure of QDs–LBD complex and sensitive response to lysozyme.

2.4. Fluorescent responses of lysozyme and other relevent substances

For fluorescent sensing of lysozyme with the as-prepared QDs–LBD probe, the QDs–LBD complex (200 nM, final concentration, representing the concentration of QDs) and different concentrations of lysozyme were added into a 1.5 mL micro-centrifuge tube containing Tris–HCl (20 mM, pH 7.4) buffer solution and the finally total volume was 1.0 mL. The mixed solution was incubated for 45 min at room temperature, and then the fluorescence intensity was monitored (excited at 365 nm). Each measurement was conducted three times.

For control experiment of selectivity, The QDs–LBD probe and the selected proteins, metal ions, or amino acids with a certain concentration were added into the Tris–HCl (pH 7.4) buffer solution with a total volume of 1.0 mL. The fluorescence intensity was measured.

2.5. Gel electrophoresis

Gel electrophoresis was conducted to confirm the binding of CA–QDs with the LBD or QDs–LBD with lysozyme. The gel was prepared containing 0.5% agarose and 1 × TB (without EDTA) with pH 8.3. A volume of 20 μL of tested samples containing 1.0% glycerol were added to each lane. The gel was run at 60 V for 40 min at room temperature. The running buffer also contained 1 × TB. The photograph was taken by EC3 imaging system under the UV-irradiation of 365 nm after exposure for 5 s.

2.6. Steady-state fluorescence anisotropy detection.

For anisotropy measurements, r, of the test solution was calculated by the following Eq. (1) [42] with the emission polarizer set at a parallel I_{vv} or perpendicular I_{vh} orientation with respect to the vertical excitation polarizer.

$$r = \frac{I_{vv} - GI_{vh}}{I_{vv} + 2GI_{vh}} \quad (1)$$

The G factor, accounting for the different sensitivities of the detected system for vertically and horizontally polarized light, was obtained by calculating the ratio of light intensities with vertical and horizontal orientation with respect to the horizontal excitation polarizer, I_{hv}/I_{hh}, which gave a value of 0.54.

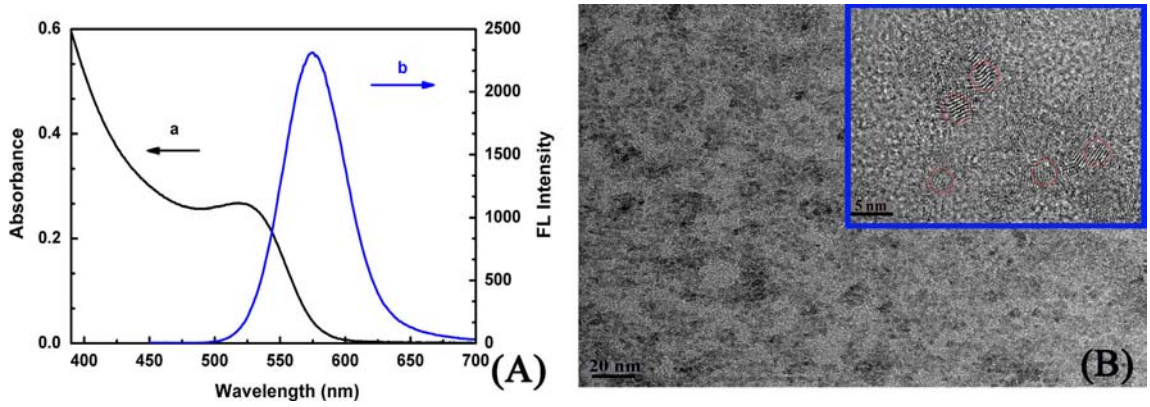

Fig. 1. (A) UV–visible absorption (a) and fluorescence emission (b) spectra of the prepared CA–capped CdTe QDs (the excitation wavelength is 365 nm). (B) TEM images of CA–CdTe QDs.

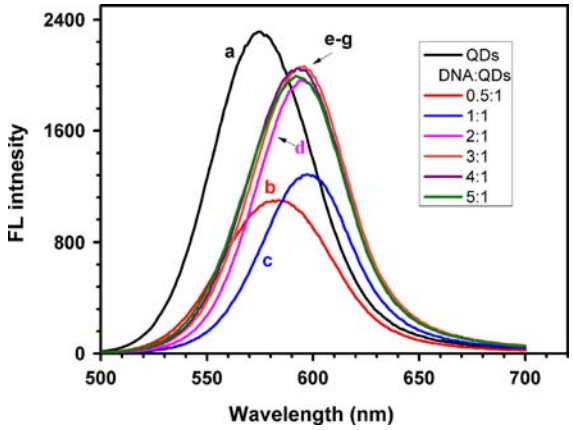

Fig. 2. Fluorescence spectra of CdTe QDs (200 nM) with different amounts of LBD added. The excitation wavelength is 365 nm.

3. Results and discussion

3.1. Characterization of CdTe QD

The UV–visible absorption spectra and fluorescence spectra of the prepared CA–CdTe QDs are shown in Fig. 1A. The maxium absorption of the first electronic transition was at 525 nm. A well-resolved maximum emission peak at 572 nm could be observed and a narrow full width at half maximum indicated a sufficiently narrow size distribution of the as-prepared CdTe QDs. The transmission electron micrograph (TEM) in Fig. 1B showed that the as-prepared CdTe QDs capped with cysteamine were well dispersed and the crystallinity of CdTe QDs was confirmed (Fig. 1B, inset). The average diameter of the CdTe QDs nanoparticles obtained by polynomial fitting function [43] was ~3.1 nm.

3.2. Binding of CA–CdTe QDs with LBD

To examine the interactions between negatively charged LBD and the positively charged CA–CdTe QDs, a titration experiment with different concentrations of LBD added into Tris–HCl buffered solution (pH 7.4) of CA–QDs was conducted, and fluorescence intensity was monitored at a fixed time interval of 10 min after addition of LBD. As shown in Fig. 2, the maximum emission wavelength of CA–CdTe QDs was at 572 nm (λ_{ex}=365 nm) giving a strong emission signal (Fig. 2, curve a). The emission intensity of CA–QDs (200 nM) decreased much when 100 nM of LBD was added (Fig. 2, curve b), but restored a little accompanying with an obvious red shift of the maximum emission wavelength to 592 nm when 200 nM of LBD was added (Fig. 2, curve c), and then restored a lot (nearly to the initial intensity of QDs itself) when the LBD concentration was increased to 400 nM (Fig. 2, curve d). And the fluorescence intensity remained unchanged when the LBD concentration was over 400 nM (Fig. 2, curve e–g). So a molar ratio of QDs to LBD of 1: 2 was chosen for the following study.

To further explore the interactions between CA–QDs and LBD, zeta potential and DLS of CA–QDs and QDs–LBD were measured. As shown in Fig. 3, upon the addition of 200 nM LBD, the average zeta potential of the CA–QDs (Fig. 3A) decreased significantly from +29.5 mV to −2.6 mV (Fig. 3B), which suggested the effective electrostatic binding between CA–QDs and LBD and the apparent surface charge was changed. It was deemed that the addition of LBD could counteract the positive charge of CA–QDs to some extent and decrease the inter-particle electrostatic repulsion which resulted in an aggregation of the particles and evident fluorescence self-quenching of the QDs nanoparticles [44,45]. With increasing the concentration of LBD, the surface zeta potential of the QDs–LBD particles changed from −2.6 mV to −19.7 mV (Fig. 3C), which suggested that more LBD bound onto the QDs surface and further changed the surface charge of the particles. And the increased negative charge on the surface dispersed the particles and made a fluorescence restoration of the QDs. The obvious changes of particle size were observed in DLS measurement when LBD was added into the solution of CA–QDs. The hydrodynamic diameter of the CA–QDs increased from 3.7 ± 1.1 nm to 34.5 ± 5.7 nm when 1 equivalent of LBD was added (Fig. 3B'). And the particle size changed to 18.8 ± 3.4 nm when 2 equivalent of LBD was added (Fig. 3C'). All the above results indicated that LBD could bind strongly with CA–QDs via electrostatic adsorption interactions. The changes of particle size together with surface charge were responsible for the fluorescence emission properties of the QDs particles [46,47].

3.3. Mechanism studies on the interactions between CA–CdTe QDs–LBD and lysozyme

In our protocol for the detection of lysozyme with QDs–LBD complex, the LBD was employed as the capture element, allowing the resulting QDs–LBD probe to bind with protein of lysozyme specifically. The sensing mechanism was described in Scheme 1. In pH 7.4, the cationic nature of the functional amino group on the QDs surface allows the CA–capped CdTe QDs to form a complex with negatively charged LBD via electrostatic interactions. When lysozyme was added, the LBD on the QDs surface coupled specifically with lysozyme to form a ternary complex of lysozyme–LBD–QDs and induced fluorescence enhancement. Unlike previous reports which was based on the competitive reaction

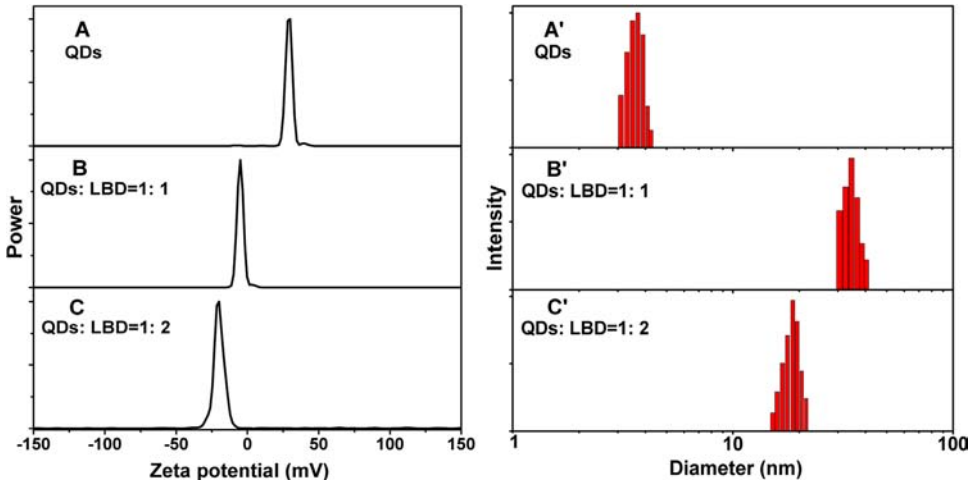

Fig. 3. Zeta potential and DLS measurement of cysteamine capped-CdTe QDs (200 nM) and QDs–LBD complex prepared at different molar ratios of QDs to LBD.

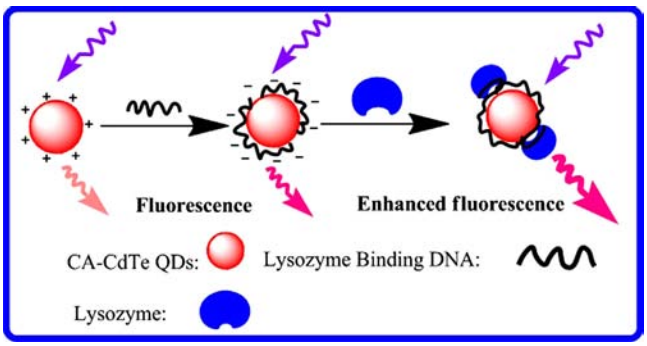

Scheme 1. Schematic illustration of the formation of QDs–LBD complex and the ternary complex of QDs–LBD–lysozyme. (Note that the sizes of substances do not represent their real proportion).

between protein/QDs with aptamers [8,48], no release of QDs was observed when LBD bound with its target lysozyme.

The formation of LBD-bridged ternary complex of QDs–LBD–lysozyme was first confirmed by fluorescence anisotropy determination. The fluorescence emission of QDs is highly isotropic in an isotropic liquid. However, the coupling of biomolecules with QDs or adsorption of biomolecules onto the surface of QDs may bring a significantly increased anisotropy signal, allowing direct monitoring of the coupling/adsorption process [49,50]. Therefore, the steady-state anisotropy of QDs, QDs–LBD and QDs–LBD–lysozyme were measured in our study. The anisotropy signal of QDs is only 0.025 for r value, and that of QDs–LBD which is a bit higher than QDs itself is 0.032. The relatively low signal of QDs and QDs–LBD can be attributed to the independent rotational movement of QDs and demonstrated that the adsorption of LBD on the surface of QDs had little effect on its anisotropy property. Due to the LBD on the QDs surface, the specific binding of lysozyme onto the QDs–LBD surface inhibited the rotational movement of QDs, thus a significantly increased anisotropy signal was observed with r value of 0.068 (nearly 3 times to the signal of free QDs, and 2 times to that of QDs–LBD). In addition, the zeta potential of QDs–LBD complex changed from −19.7 mV to −11.26 mV as a result of lysozyme binding (Fig. S1).

The binding model was also proved by agarose gel electrophoresis. As shown in Fig. 4, the free CA–CdTe QDs was unable to move towards the positive electrode due to the positive charge on the CA–QDs surface (lane A). However, when the sample of QDs–LBD was loaded, an obvious light band was observed, indicating the binding between CA–QDs and LBD and negative charge on the whole particle (lane B). In the presence of lysozyme, the ternary

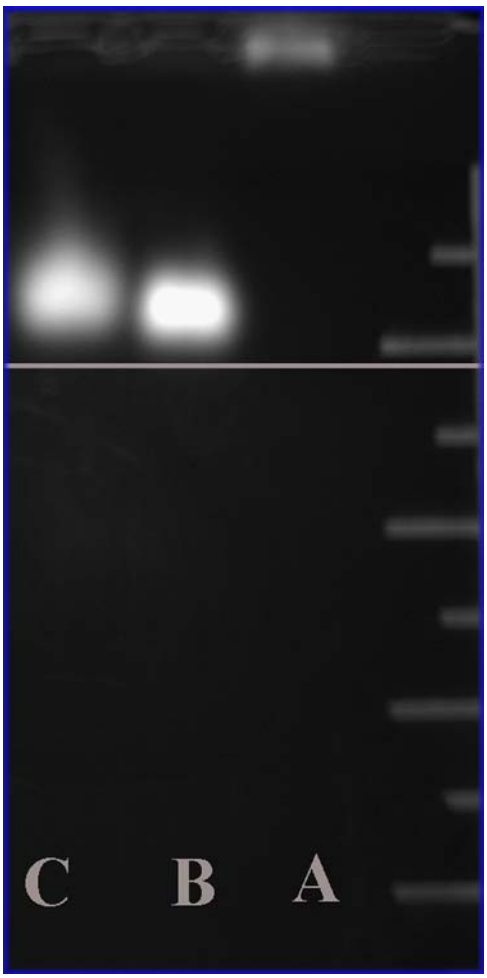

Fig. 4. The agarose gel electrophoresis results of CA–QDs, QDs–LBD and QDs–LBD–lysozyme. From right to left: lane A: 200 nM CA–QDs; lane B: QDs–LBD (QDs: LBD=1: 2); and lane C: QDs–LBD complex interacted with 62.3 nM of lysozyme.

mixture behaved in a manner similar to that of QDs–LBD complex in the gel electrophoresis but exhibited a bit slow-moving band (lane C), and this suggested the formation of LBD-bridged ternary complex of QDs–LBD–lysozyme which had a relatively larger mass and less negative charge compared with the QDs–LBD complex [51–53]. These results strongly supported that QDs, LBD and lysozyme would form a LBD-bridged ternary complex.

3.4. Fluorescent sensing of lysozyme with QDs–LBD probe

As previous study indicated [54], the interactions between LBD and protein depended on incubation time. For lysozyme sensing, the effect of incubation time was studied via monitoring the fluorescence intensity changes of QDs–LBD complex when lysozyme was added after a certain time interval. From Fig. S2, it can be seen that the fluorescence intensity ratio F/F_0 (F and F_0 referred to the fluorescence intensity of QDs–LBD in the presence and absence of lysozyme) increased sharply in the first 30 min of incubation, and then increased slowly after 45 min. So it was deemed that the specific binding interactions between lysozyme and QDs–LBD complex achieved completion within 45 min.

The effect of pH on the interactions between lysozyme and QDs–LBD complex was also studied. As shown in Fig. S3, the fluorescence intensity ratio, F/F_0, varied with the variation of pH and reached the highest at pH 7.4. It was speculated that, the conjugation of positively charged amino group on the surface of CdTe QDs with the negatively charged LBD which could form a compact and stable QDs–LBD complex was critical for the formation of ternary complex of QDs–LBD–lysozyme.

The ionic strength would also influence the interactions between QDs–LBD complex and lysozyme, and this was studied by varying NaCl concentration of the system and monitoring the fluorescence changes when lysozyme interacted with QDs–LBD complex. As shown in Fig. S4, at certain concentration of QDs–LBD complex (200 nM) and lysozyme (35.6 nM), 8.5 mM NaCl was the tolerable concentration for a satisfying response.

For sensing of lysozyme, different concentrations of lysozyme were added into the Tris–HCl buffered solution (pH 7.4, with 8.5 mM NaCl) containing QDs–LBD complex and the fluorescence intensity was monitored after incubation of 45 min. As previously described, addition of lysozyme to the solution of QD–LBD complex could lead to the fluorescence enhancement of the QDs due to the adsorption of lysozyme on the surface of the QDs–LBD. The changes in surface and electrostatic properties will likely affect the efficiency of core electron–hole recombination and lead to the observed fluorescence enhancement [55,56]. As shown in Fig. 5, the fluorescence intensity of the QDs–LBD increased gradually when the concentration of lysozyme varied from 8.9 to 71.2 nM, and then followed a slow rise at higher concentration over 71.2 nM. The inset calibration curve depicted the resulting relationship between the fluorescence changes at 592 nm and lysozyme concentration. A good linear relationship was found between $(F-F_0)/F_0$ (F and F_0 are the fluorescence intensity of QDs–LBD complex in the presence and absence of lysozyme, respectively) and the lysozyme concentration in the range of 8.9–71.2 nM with a detection limit (LOD) of 4.3 nM (the detection limit is defined by the equation $\mathrm{LOD}=3\sigma/s$, where σ is the standard deviation of the corrected blank signals of the QDs–LBD complex ($n=11$) and s is the slope of the calibration curve). The regression equation is $(F-F_0)/F_0=0.00747C$ (nM)$+1.0075\times10^{-4}$ ($R^2=0.996$). The binding ratio of lysozyme to QDs–LBD was estimated to be 2: 1 by α fitting analysis (Fig. S5) [57], which was consistent with the previous study by Willson [36]. That was a 1: 2: 2 ternary complex of QDs: LBD: lysozyme was formed.

In addition, we also confirmed that there were no obvious interactions between lysozyme and native CA–CdTe due to the electrostatic repulsion between lysozyme and CA–CdTe (Fig. S6). It was deemed that LBD on the surface of QDs acted as the bridge to bring the specific lysozyme target and QDs–LBD probe into proximity and induced the increase of fluorescence intensity of QDs.

To investigate the selectivity of this QDs–LBD probe for lysozyme recognition, a control experiment was carried out by testing lysozyme as well as other proteins. Lysozyme has a primary sequence of 129 amino acids with a molecular weight (M_w) of 14,400 and an isoelectric point (pI) of 11.0 [58]. The four non-specific proteins with different molecular weights (M_w) and isoelectric points (pI) are thrombin (M_w: 23.3 kDa, pI: 6.4–7.6), bovine serum albumin (BSA) (M_w: 66 kDa, pI: 4.7), IgG (M_w: 150 kDa, pI: 4.7–5.5), and trypsin (M_w: 23.3 kDa, pI: 10.1–10.5). At pH 7.4, thrombin has neutral charge, BSA and IgG are negatively charged, and trypsin and lysozyme are positively charged, respectively. As was demonstrated in Fig. 6, there were significant differences in the fluorescence intensity changes when lysozyme and other proteins (thrombin, BSA, IgG or trypsin) were added into the solution of QDs–LBD. Only lysozyme can induce a remarkable fluorescence enhancement of the QDs–LBD complex, while the other proteins could only induce a slight increase of the fluorescence signal. In addition, the responsiveness of the biosensor for lysozyme in the presence of a mixture of other proteins was also examined. The $(F-F_0)/F_0$ value obtained from the response of QD–LBD complex to 35 nM of lysozyme in the presence of high concentrations of other possible interfering proteins (175 nM in total) had no apparent difference with that obtained in the absence of interfering proteins, indicating that the other co-existed proteins had negligible influence on the lysozyme detection.

Furthermore, the effect of some bio-related species on the detection of lysozyme was also studied. Table S1 gave the tolerable

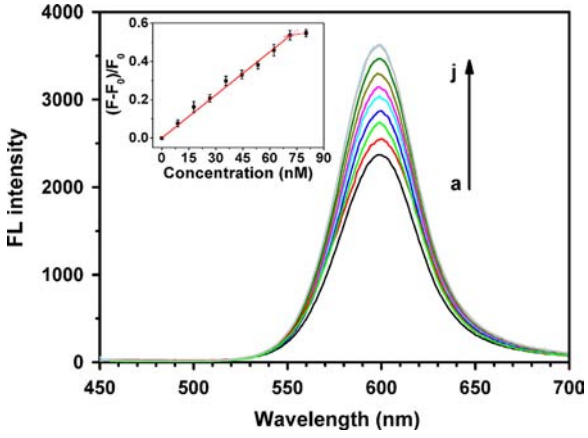

Fig. 5. The fluorescence spectra of 200 nM QDs–LBD complex in the presence of different concentrations of lysozyme ((a) 0; (b) 8.9; (c) 17.8; (d) 26.7; (e) 35.6; (f) 44.5; (g) 53.4; (h) 62.3; (i) 71.2; (j) 90.1 nM). Inset graph: relationship between the fluorescence intensity of QDs–LBD complex and different concentrations of lysozyme. F and F_0 are the fluorescence intensities of QDs–LBD complex at 592 nm in the presence and absence of lysozyme, respectively. The excitation wavelength is 365 nm.

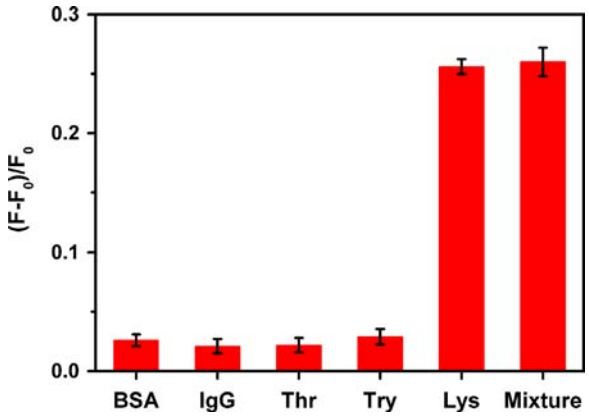

Fig. 6. Responses of QDs–LBD probe (200 nM, representing the concentration of QDs) to different proteins studied: BSA, 36.5 nM; IgG, 30.0 nM; Thr, 35.0 nM; Try, 39.0 nM; Lys, 35.6; Mixture, lysozyme (35.6 nM) and other proteins (BSA, 36.5 nM; IgG, 30.0 nM; Thr, 35.0 nM; Try, 39.0 nM) co-existed. F and F_0 are the fluorescence intensities of QDs–LBD complex at 592 nm in the presence and absence of proteins, respectively. The excitation wavelength is 365 nm.

Table 1
The results of lysozyme detection in mouse serum and human morning urine sample.

Sample	Found in diluted sample (nM)	Added (nM)	Totally found (nM)	Recovery (%)	RSD[c] (%)
1[a]	9.3	17.5	27.9	106.3	4.3
2[a]	10.1	35.0	44.2	97.4	1.1
3[a]	9.5	52.5	58.2	92.8	5.3
1[b]	–	17.5	18.7	107.2	3.1
2[b]	–	35.0	34.8	99.4	4.2
3[b]	–	70.0	70.9	101.4	6.2

[a] Serum sample.
[b] Urine sample.
[c] Each sample was repeated for three times independently and averaged to obtain the recovery and RSD values.

concentration of some inorganic ions and amino acids by the criterion which gave a relative error of less than 10% for the determination of 35.6 nM lysozyme. The tolerable concentration ratios of coexisting substance to 35.6 nM lysozyme was over 2.5×10^5-fold for inorganic ions, and 3.0×10^5-fold for amino acids. These results showed that there were little interferences from commonly coexisting substances. The approach developed here displayed high selectivity for the determination of lysozyme.

3.5. Determination of lysozyme in serum and human morning urine

To demonstrate the potential application of the proposed method for lysozyme analysis in biological media, the assay of lysozyme in mouse serum and human morning urine (urine was freshly taken from human and was centrifuged at 6000 rpm for 20 min to get the supernatant) was performed. Specifically, different concentrations of lysozyme were added into the 30-fold diluted serum and 20-fold diluted urine samples, and the fluorescence spectra and the lysozyme concentration detected are shown in Fig. S7 and Table 1, respectively. From Table 1, it can be seen the recovery of added lysozyme detected in the spiked serum samples ranged from 92% to 106%, and the relative standard deviations were no more than 6%. The recovery of added lysozyme detected in morning urine samples ranged from 99% to 107%, and the relative standard deviations were between 3.1% and 6.2%. The above results suggested that the proposed approach had potential bio-medical application since the abnormal lysozyme level in serum and urine indicates some diseases.

4. Conclusions

In summary, a facile approach for fluorescent sensing of lysozyme was demonstrated using CdTe QDs and lysozyme binding DNA (LBD) as a probe. The negatively charged LBD could conjugate with the positively charged CA–capped CdTe QDs forming a stable complex. While in the presence of lysozyme, the QDs–LBD complex could bind specifically with lysozyme to form a 1: 2: 2 ternary complex of QDs–LBD–lysozyme, and fluorescence enhancement of the QDs was observed. The binding mechanism was also confirmed by zeta potential and dynamic light scattering measurement as well as gel electrophoresis experiment. This method was simple, easy to operate, and offered comparable sensitivity compared with previously reported method for lysozyme detection. In addition, the QDs–LBD probe had highly selective response to lysozyme over other proteins and could tolerate high concentration of biologically relevant inorganic ions and amino acid. The method was also successfully applied to lysozyme detection in biological samples of serum and urine with good recovery.

Acknowledgments

This project was supported by the National Natural Science Foundation of China (No. 20905008), and the Fundamental Research Funds for the Central Universities (No. 2012LYB17).

Appendix A. Supporting information

Supplementary data associated with this article can be found in the online version at http://dx.doi.org/10.1016/j.talanta.2014.04.062.

References

[1] S.S. Levinson, R.J. Elin, L. Yam, Clin. Chem. 48 (2002) 1131–1132.
[2] J.F. Harrison, G.S. Lunt, P. Scott, J.D. Blainey, Lancet 1 (1968) 371–375.
[3] J. Ireland, J. Herzog, E.R. Unanue, J. Immunol. 177 (2006) 1421–1425.
[4] C. Tuerk, L. Gold, Science 249 (1990) 505–510.
[5] A.D. Ellington, J.W. Szostak, Nature 346 (1990) 818–822.
[6] A.D. Kent, N.G. Spiropulos, J.M. Heemstra, Anal. Chem. 85 (2013) 9916–9923.
[7] D.M. Engelhard, R. Pievo, G.H. Clever, Angew. Chem. Int. Ed. 52 (2013) 12843–12847.
[8] W.L. Sun, T.M. Yao, S. Shi, Analyst 137 (2012) 1550–1552.
[9] Matthew Levy, S.F. Cater, A.D. Ellington, ChemBioChem 6 (2005) 2163–2166.
[10] K. Gang-Il, K. Kyung-Woo, O. Min-Kyn, S. Yun-Mo, Nanotechnology 20 (2009) 175503-1–175503-5.
[11] X.Q. Liu, R. Freeman, E. Golub, I. Willner, ACS Nano 5 (2011) 7648–7655.
[12] J.C. Cox, A.D. Ellington, Bioorg. Med. Chem. 9 (2001) 2525–2531.
[13] A.-N. Kawde, M.C. Rodriguez, T.M.H. Lee, J. Wang, Electrochem. Commun. 7 (2005) 537–540.
[14] M.C. Rodriguez, A.N. Kawde, J. Wang, Chem. Commun. (2005) 4267–4269.
[15] A.K.H. Cheng, B.X. Ge, H.Z. Yu, Anal. Chem. 79 (2007) 5158–5164.
[16] J. Wang, B. Liu, Chem. Commun. (2009) 2284–2286.
[17] P. Zhong, Y. Yu, J.Z. Wu, Y. Lai, B. Chen, Z.Y. Long, C.S. Liang, Talanta 70 (2006) 902–906.
[18] D. Tang, D.L. Liao, Q.K. Zhu, F.Y. Wang, H.P. Jiao, Y.J. Zhang, C. Yu, Chem. Commun. 47 (2011) 5485–5487.
[19] C.F. Chen, J.J. Zhao, J.H. Jiang, R.Q. Yu, Talanta 101 (2012) 357–361.
[20] D.L. Liao, J. Chen, W.Y. Li, Q.F. Zhang, F.Y. Wang, Y.X. Li, C. Yu, Chem. Commun. 49 (2013) 9458–9460.
[21] P. Kara, A. Escosura-Muñiz, M.M. Costa, M. Guix, M. Ozsoz, A. Merkoci, Biosens. Bioelectron. 26 (2010) 1715–1718.
[22] Z.B. Chen, L.D. Li, H.T. Zhao, L. Guo, X.J. Mu, Talanta 83 (2011) 1501–1506.
[23] J.X. Guo, Electrochim. Acta 111 (2013) 916–920.
[24] Z.B. Chen, J.X. Guo, J. Li, L. Guo, RSC Adv. 3 (2013) 14385–14389.
[25] Y.H. Xiao, Y.P. Wang, M. Wu, X.L. Ma, X.D. Yang, J. Electroanal. Chem. 702 (2013) 49–55.
[26] H.P. Huang, G.F. Jie, R.J. Cui, J.J. Zhu, Electrochem. Commun. (2009) 816–818.
[27] H.Y. Wang, W. Gong, Z.A. TanX.X. YinL. Wang, Electrochim. Acta 76 (2012) 416–423.
[28] Y.G. Peng, D.D. Zhang, Y. Li, H.L. Qi, Q. Gao, C.X. Zhang, Biosens. Bioelectron. 25 (2009) 94–99.
[29] L.Q. Wang, L.Y. Li, Y. Xu, G.F. Cheng, P.G. He, Y.Z. Fang, Talanta 79 (2009) 557–561.
[30] S. Bamrungsap, M.I. Shukoor, T. Chen, K. Sefah, W.H. Tan, Anal. Chem. 83 (2011) 7795–7799.
[31] Y.M. Chen, C.J. Yu, T.L. Cheng, W.L. Tseng, Langmuir 24 (2008) 3654–3660.
[32] M. Girardot, S. Descroix, A. Varenne, Anal. Biochem. 435 (2013) 150–152.
[33] P. Subramanian, A. Lesniewski, I. Kaminska, A. Vlandas, R. Boukherroub, Biosens. Bioelectron. 50 (2013) 239–243.
[34] C.F. Chen, J.J. Zhao, J.H. Jiang, R.Q. Yu, Talanta 101 (2012) 357–361.
[35] P. Subramanian, A. Lesniewski, I. Kaminska, A. Vlandas, A. Vasilescu, J. Niedziolka-Jonsson, E. Pichonat, H. Happy, R. Boukherroub, S. Szunerits, Biosens. Bioelectron. 50 (2013) 239–243.
[36] A.S.R. Potty, K. Kourentzi, H. Fang, P. Schuck, R.C. Willson, Int. J. Biol. Macromol. 48 (2011) 392–397.
[37] P.L. Truong, S.P. Choi, S.J. Sim, Small 20 (2013) 3485–3492.
[38] G.X. Jiang, A.S. Susha, A.A. Lutich, F.D. Stefani, J. Feldmann, A.L. Rogach, ACS Nano 3 (2009) 4127–4131.
[39] T. Li, R. Fu, H.G. Park, Chem. Commun. 46 (2010) 3271–3273.
[40] P. Song, Y. Xiang, H. Xing, Z. Zhou, A. Tong, Y. Lu, Anal. Chem. 84 (2012) 2916–2922.
[41] N. Gaponik, D.V. Talapin, A.L. Rogach, K. Hoppe, E.V. Shevchenko, A. Kornowski, A. EychmÜller, H. Weller, J. Phys. Chem. B 106 (2002) 7177–7185.
[42] T. Ozel, S. Nizamoglu, M.A. Sefunc, O. Samarskaye, I.O. Ozel, E. Mutlugun, V. Lesnyak, N. Gaponik, A. Eyclmuller, S.V. Gaponenko, H.V. Demir, ACS Nano 5 (2011) 1328–1334.
[43] W.W. Yu, L.H. Qu, W.Z. Guo, X.G. Peng, Chem. Mater. 15 (2003) 2854–2860.
[44] I.L. Medintz, L. Berti, T. Pons, A.F. Grimes, D.S. English, A. Alessandrini, P. Facci, H. Mattoussi, Nano Lett. 7 (2007) 1741–1748.
[45] D.Z. Sun, O. Gang, Langmuir 29 (2013) 7038–7046.

[46] Y.Q. Li, J.H. Wang, H.L. Zhang, J. Yang, L.Y. Guang, H. Chen, Q.M. Luo, Y.D. Zhao, Biosens. Bioelectron. 25 (2010) 1283–1289.
[47] H.Y. Liu, S.M. Xu, Z.M. He, A.P. Deng, J.J. Zhu, Anal. Chem. 85 (2013) 3385–3392.
[48] Y.Z. Xiang, R.X. Hu, N. Shao, Talanta 107 (2013) 140–145.
[49] M.J. Zou, Y. Chen, X. Xu, H.D. Huang, F. Liu, N. Li, Biosens. Bioelectron. 32 (2012) 148–154.
[50] G. Giraud, H. Schulze, T.T. Bachmann, C.J. Campbell, A.R. Mount, P. Ghazal, M.R. Khondoker, S.W.J. Ember, I. Ciani, C. Tlili, A.J. Walton, J.G. Terry, J. Crain, Chem. Phys. Lett. 484 (2010) 309–314.
[51] Y. Liu, M.X. Zhang, Z.L. Zhang, H.Y. Xie, Z.Q. Tian, K.Y. Wong, D.W. Pang, Front. Biosci. 13 (2008) 923–928.
[52] L. Berti, P.S.D. Agostino, K. Boeneman, I.L. Medintz, Nano Res. 2 (2009) 121–129.
[53] J.H. Liu, C.Y. Wang, Y. Jiang, Y.P. Hu, J.S. Li, S. Yang, Y.H. Li, R.H. Yang, W.H. Tan, C.Z. Huang, Anal. Chem. 85 (2013) 1424–1430.
[54] Y.H. Chen, L. Wang, W. Jiang, Talanta 97 (2012) 533–538.
[55] H. Mattoussi, J.M. Mauro, E.R. Goldman, G.P. Anderson, V.C. Sundar, F.V. Mikulec, M.G. Bawendi, J. Am. Chem. Soc. 122 (2000) 12142–12150.
[56] M. Idowu, E. Lamprecht, T. Nyokong, J. Photochem. Photobiol. A: Chem. 198 (2008) 7–12.
[57] R.H. Yang, W.H. Chan, A.W.M. Lee, P.F. Xia, H.K. Zhang, K.A. Li, F. Liu, J. Am. Chem. Soc. 125 (2003) 2884–2885.
[58] D.J. Vocadlo, G.J. Davies, R. Laine, S.G. Withers, Nature 412 (2001) 835–838.